Journal of Medicinal Chemistry

Article

pubs.acs.org/jmc

In Silico Discovery of a Compound with Nanomolar Affinity to Antithrombin Causing Partial Activation and Increased Heparin Affinity

J. Navarro-Fernández,[†,∥] H. Pérez-Sánchez,[‡,§,∥] I. Martínez-Martínez,[†] I. Meliciani,[‡] J. A. Guerrero,[†] V. Vicente,[†] J. Corral,*[,†] and W. Wenzel*[,‡]

[†]Servicio de Hematología y Oncología Médica, H. U. Morales Meseguer, Centro Regional de Hemodonación, University of Murcia, Spain

[‡]Institute of Nanotechnologie, Karlsruhe Institute of Technology, Karlsruhe, Germany

[§]Department of Computer Engineering, School of Computer Science, University of Murcia, Spain

Supporting Information

ABSTRACT: The medical and socioeconomic relevance of thromboembolic disorders promotes an ongoing effort to develop new anticoagulants. Heparin is widely used as activator of antithrombin but incurs side effects. We screened a large database in silico to find alternative molecules and predicted D-myo-inositol 3,4,5,6-tetrakisphosphate (TMI) to strongly interact with antithrombin. Isothermal titration calorimetry confirmed a TMI affinity of 45 nM, higher than the heparin affinity (273 nM). Functional studies, fluorescence analysis, and citrullination experiments revealed that TMI induced a partial activation of antithrombin that facilitated the interaction with heparin and low affinity heparins. TMI improved antithrombin inhibitory function of plasma from homozygous patients with antithrombin deficiency with a heparin binding defect and also in a model with endothelial cells. Our in silico screen identified a new, non-polysaccharide scaffold able to interact with the heparin binding domain of antithrombin. The functional consequences of this interaction were experimentally characterized and suggest potential anticoagulant therapeutic applications.

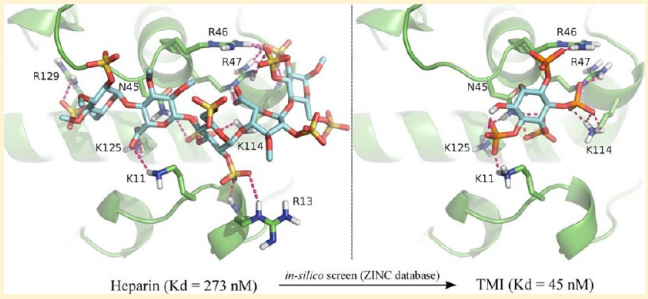

INTRODUCTION

Ever since the discovery of the anticoagulant properties of hirudin from the leech saliva, the increasing relevance of thromboembolic diseases has encouraged a continuous search for new compounds with anticoagulant activity, which has led to the development of the new commercially available anticoagulants.[1] One of the targets for prophylaxis and treatment of thromboembolic diseases is the plasma anticoagulant antithrombin. Antithrombin is a member of the serpin superfamily of protease inhibitors. As in other serpins, antithrombin inhibits its proteases by an unusual branched pathway suicide substrate mechanism in which the reactive center loop of the inhibitor is cleaved by the protease as a normal substrate but is trapped as an acyl intermediate covalent complex.[2,3] However, antithrombin circulates in blood in a metastable conformation in which the reactive center loop is partially inserted and is only activated by heparin and heparan sulfate glycosaminoglycans on the injured subendothelium.[4−6] Accordingly sulfated polysaccharide heparin chains with different size, from unfractionated to the essential pentasaccharide, have been used successfully in anticoagulant therapy and thromboprophilaxis.[7]

Since the discovery of the anticoagulant activity of heparins isolated from canine liver in 1916,[8] several new molecules able to bind antithrombin have been identified. The strategies used in this search have been based mainly on the synthesis or chemical modification of existing drugs or in the application of natural compounds with properties similar to those currently used.[9] Examples of such compounds are lignins and flavonoids,[9,10] highly sulfated small organic ligands that seem to have similar properties to heparins. An alternative approach is to screen a large database in silico and use affinity-ranking to identify some at least weakly binding molecules for further refinement. Aided by ever-increasing computational power,[11,12] virtual screening is an appealing and cost-effective approach to tap into the wealth of available structural information.[13] However, despite several success stories, limitations in current in silico screening approaches restrict their accuracy and general applicability.[14,15]

Here we have pursued an in silico discovery strategy in order to find molecules with non-polysaccharide scaffolds in the ZINC database[16] with strong interactions with the heparin binding domain of antithrombin. The ligand with highest score, D-myo-inositol 3,4,5,6-tetrakisphosphate (TMI), was experimentally validated confirming that this compound binds to

Received: March 20, 2012
Published: June 28, 2012

dx.doi.org/10.1021/jm300621j | J. Med. Chem. 2012, 55, 6403−6412

antithrombin with nanomolar affinity. Moreover, the functional consequences of such interaction were investigated and the potential therapeutic relevance was discussed.

RESULTS

Validation of in Silico Models for Heparin–Antithrombin Binding. A prerequisite of a successful in silico screen is the reproduction of the experimental binding pose of known ligands, which is difficult for heparin, as it contains five saccharide rings with more than 200 atoms and more than 60 flexible bonds. Using the docking protocol detailed in the Experimental Section, we were able to reproduce the experimental binding pose of heparin complexed with antithrombin to within 0.2 Å rmsd with reference to the crystal structure (PDB code 1AZX; see Figure 1). In the binding pose we observe strong electrostatic interactions between oxygens from sulfo groups of heparin and positively charge residues from antithrombin and hydrogen bonds (detailed in Table 1) as depicted in Figure 2A, which helps in the subsequent high-throughput screen because such interactions are well represented by the force-field-based scoring function.

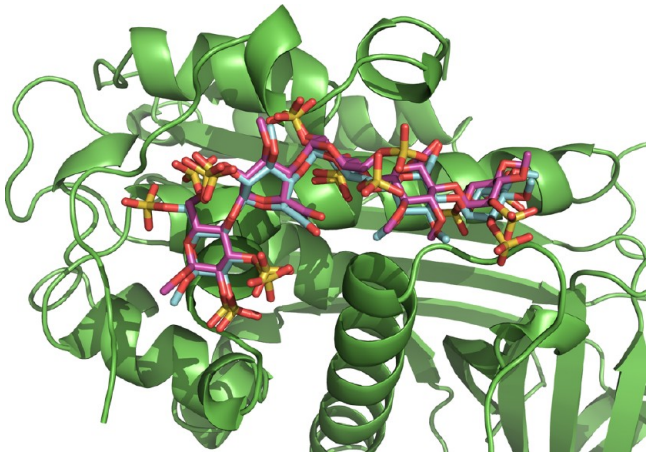

Figure 1. Overlay of the predicted and experimental binding mode of heparin with antithrombin. Blue and yellow color poses correspond to the experimental and predicted binding modes, respectively.

In Silico Discovery of Antithrombin High-Affinity Compounds. We used a surface screening analysis (Figure 3) to select an area over the antithrombin surface that belongs to the heparin binding site for docking of chemical compounds from the ZINC database. After screening 13 million compounds with FlexScreen (see Experimental Section), we selected four compounds with a score close to that calculated for heparin. D-Myo-inositol 3,4,5,6-tetrakisphosphate (TMI) was predicted to have the best binding energy of the molecules on the list (Table 1). The binding poses of these compounds onto heparin binding site in antithrombin are shown in Figure 2. In order to validate the interaction of these compounds, we explored the whole surface of antithrombin using surface screening (see Experimental Section) in order to identify potentially competing binding sites. We found unequivocally that the binding site with the strongest interactions was always the heparin-binding area, even though there are other areas where the molecule may bind weakly, as shown in Figure 4 for TMI as an example. The binding mode of TMI predicted by FlexScreen is the same area as heparin (Figure 4).

To validate the interactions observed in silico, we performed isothermal titration calorimetry (ITC) experiments with the four selected compounds. Of the compounds investigated only TMI interacted with antithrombin. Interestingly, this interaction was 6-fold stronger (45 nM) than that measured for pentasaccharide (273 nM) (Figure 5A and Figure 5B). Analyzing the interactions in detail, we found a high similarity between the stabilizing electrostatic interaction of the phosphate groups of TMI and heparin with the strongly ionic and polar surface residues of antithrombin (see Table 1 and Figure 2A and 2D). TMI is already present in the human body,[17,18] and there are data on the use of high concentrations of myo-inositol, without observing associated side effects.[19]

TMI–Antithrombin Acts as a Strong Coactivator to Heparin. Relevance for Heparin Affinity. Next we tested the effect of TMI on antithrombin by evaluating the antithrombin and anti-FXa activity of antithrombin. TMI produced a ~3-fold increase in activity (Table 2), pointing to a possible allosteric effect of the molecule. However, the

Table 1. Ranking of Chemicals Included in the Library ZINC Database That Interact with the Heparin Binding Site of Antithrombin According to the FlexScreen Scoring Function (FS SF) Values[a]

				interacting residue								
compd	FS SF	K_d	functional group	K11	R13	N45	R46	R47	K114	K125	R129	R132
heparin	−1200	273	SO_4	ES	ES		ES	ES	ES	ES	ES	ES
				HB	HB	HB	HB	HB	HB	HB	HB	
BTCA	−966		CO_2	ES			ES	ES	ES			
								HB	HB			
TPSNDBDS	−1062		SO_4	ES			ES	ES	ES			ES
						HB			HB			HB
TMI	−2300	45	PO_4	ES			ES	ES	ES	ES		
				HB		HB	HB	HB	HB			
DHSND	−728		SO_3	ES				ES	ES	ES		
				HB		HB		HB	HB	HB		

[a]The data obtained for heparin are also included. The K_d (nM) calculated by intrinsic fluorescence analysis is also indicated. For each compound we indicate the main type of interacting functional group and the type of interaction predicted by FlexScreen with each residue by ES (strong electrostatic interactions) and HB (one or several hydrogen bonds formed). BTCA: 1,2,4-benzenetricarboxylic acid. TPSNDBDS: tetrapotassium 2,5-bis[(4-sulfonatophenyl)diazenyl]benzene-1,3-disulfonate. TMI: D-myo-inositol 3,4,5,6-tetrakisphosphate. DHADSA: disodium 4-hydroxy-5-sulfonaphthalene-2,7-disulfonate.

dx.doi.org/10.1021/jm300621j | J. Med. Chem. 2012, 55, 6403–6412

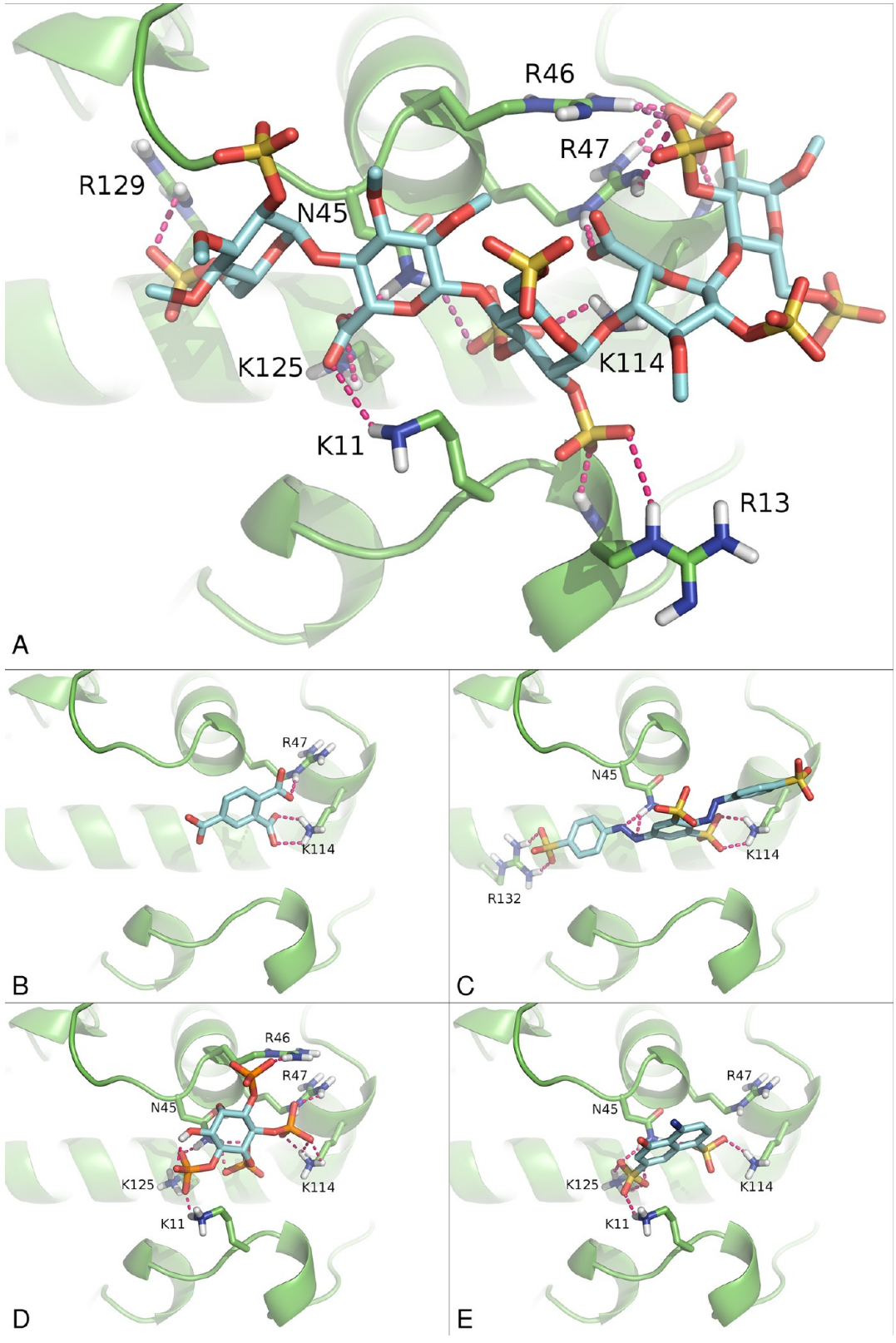

Figure 2. Representation of the binding modes obtained between antithrombin and compounds from Table 1, from up left to down right, for (A) heparin, (B) 1,2,4-benzenetricarboxylic acid, (C) tetrapotassium 2,5-bis[(4-sulfonatophenyl)diazenyl]benzene-1,3-disulfonate, (D) TMI, and (E) disodium 4-hydroxy-5-sulfonaphthalene-2,7-disulfonate. Hydrogen bonds are highlighted in magenta.

increased intrinsic fluorescence caused by the interaction of unfractionated heparin (UFH) with antithrombin was not produced when using TMI (Figure 6). As TMI and heparin are predicted to share interactions with antithrombin, we evaluated the consequences of TMI binding on the interaction of antithrombin with heparin by fluorescence analysis, observing a 2.3-fold increase in the heparin affinity of antithrombin in the presence of TMI. The K_d of heparin changed from 56 to 24

dx.doi.org/10.1021/jm300621j | J. Med. Chem. 2012, 55, 6403−6412

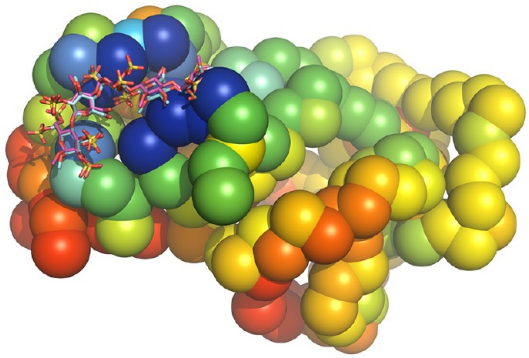

Figure 3. Representation of the predicted interacting regions resulting from the surface scan of the whole surface of antithrombin. We performed different simulations starting near the center of each colored bead, which were confined to the vicinity of each bead. The beads are colored in a rainbow scale according to the value of the scoring function for the resulting best position. Colors from red to blue denote stronger interactions. The crystallographic and predicted binding modes of heparin are shown with pink and blue color skeletons, respectively.

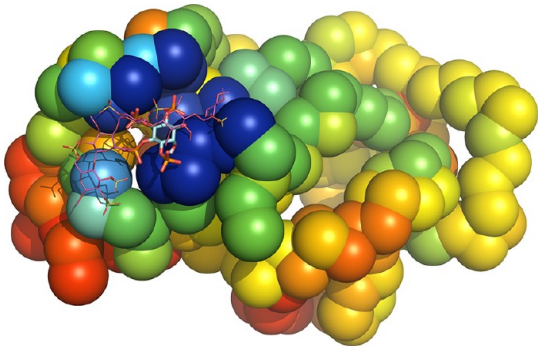

Figure 4. Representation of the docking results for TMI obtained over the whole surface of antithrombin. Each different simulation starts on the center of each colored bead. Color of each bead denotes scoring function value. Colors from red to blue denote stronger interactions. In order to emphasize location of binding site, crystallographic pose of heparin (pink skeleton) is shown. Predicted binding mode of TMI is shown in blue skeleton.

nM, in the presence of a saturating concentration of TMI (37 μM) (Figure 6C). This interesting effect was further confirmed by ITC, which indicated a 14.5-fold increase in the heparin affinity to antithrombin, from 273 nM in the absence of the compound to 18.8 nM in the presence of 37 μM TMI (Figure 5C). The discrepancy in the values obtained with these two methods (fluorescence and ITC) could be explained by the higher sensitivity of ITC, which registers effects caused by both increased interaction and conformational changes while changes in fluorescence emission are only detected when activation is achieved.

Although TMI increases the heparin affinity, the rate of inhibition of thrombin and FXa due to high affinity heparin activation of antithrombin is not affected by the presence of this compound (Table 2). In contrast, TMI caused a slight increase in these rates when the reaction was carried out in the presence of low affinity heparin (Table 2), which is the heparan sulfate that lines the vascular endothelium.

TMI Leads to Antithrombin Activation by Induced Conformational Change. The increased heparin affinity and the mild activation of antithrombin caused by TMI suggest a partial activation of antithrombin. Such activation can be verified by investigating the exposure of the antithrombin reactive loop[20] by incubating antithrombin with peptidyl arginine deiminase (PAD). This enzyme citrullinates the P1 residue of antithrombin (Arg393), inactivating the anticoagulant activity of the molecule.[21] This reaction is considerably accelerated when the P1 residue of antithrombin is exposed by activation with heparin.[22] Interestingly, TMI caused the same decrease as heparin in the anti-FXa activity when antithrombin was incubated with PAD (Table 3).

Antithrombin is a conformational sensitive serpin that rapidly incorporates the reactive center loop to reach a hyperstable conformation in response to the proteolytic cleavage of target proteases but also under even minor structural modifications caused by mutations or stress conditions.[23,24] We evaluated potential conformational effects of the interaction of TMI with antithrombin. According to native PAGE in the presence and absence of urea, up to 14.8 μM TMI at 37 or 42 °C for 2 days increased neither the transition to the latent conformation nor the formation of polymers of antithrombin (Supporting Information Figures S1 and S2).

TMI in Plasma of Patients with Heparin Binding Defect. We investigated the effect of TMI on antithrombin activity of plasma from a homozygous patient with the L99F mutation (antithrombin Budapest III), which leads to a dramatic reduction of heparin affinity. Treatment or prophylaxis with heparin in homozygous for this or similar mutations is consequently unsuccessful. Using a chromogenic method, we found that TMI induced a 19% activation of the plasma antithrombin activity from a homozygous L99F patient in the presence of UFH (Table 4). A similar activation (11%) was achieved when plasma of this patient was evaluated in a system free of exogenous heparin that used endothelial cells as a source of heparan sulfates (Table 4).

■ DISCUSSION AND CONCLUSIONS

The challenge of an aging society with anticoagulant requirements of increasing complexity encourages the search for new anticoagulant molecules. Different approaches and targets have been assayed, some of them with excellent and promising results.[25,26] In this study, we have selected antithrombin as a promising target, which is activated by heparins, and performed structure based in silico screening techniques to discover new compounds with anticoagulant effects. These methods now permit virtual screening of millions of compounds, considerably reducing experimental work and cost of wet-chemistry screening, but are not applicable to all targets.

Heparin is among the most widely used drugs in developed societies to prevent or treat thromboembolic diseases. Unfortunately, because of its highly anionic nature, heparin is involved in many interactions with blood proteins other than antithrombin and with vessel wall components[27] that can be involved in an appreciable individual variability in optimal dosage and an associated risk for bleeding complications. Moreover, such interactions may also lead to side effects like thrombocytopenia and osteoporosis.[28−30] These problems have inspired efforts to design safer and more specific therapeutic agents that would be free of such complications, but undesired effects remain for all presently available alternatives. Development of low molecular weight heparins (LMWHs), which are

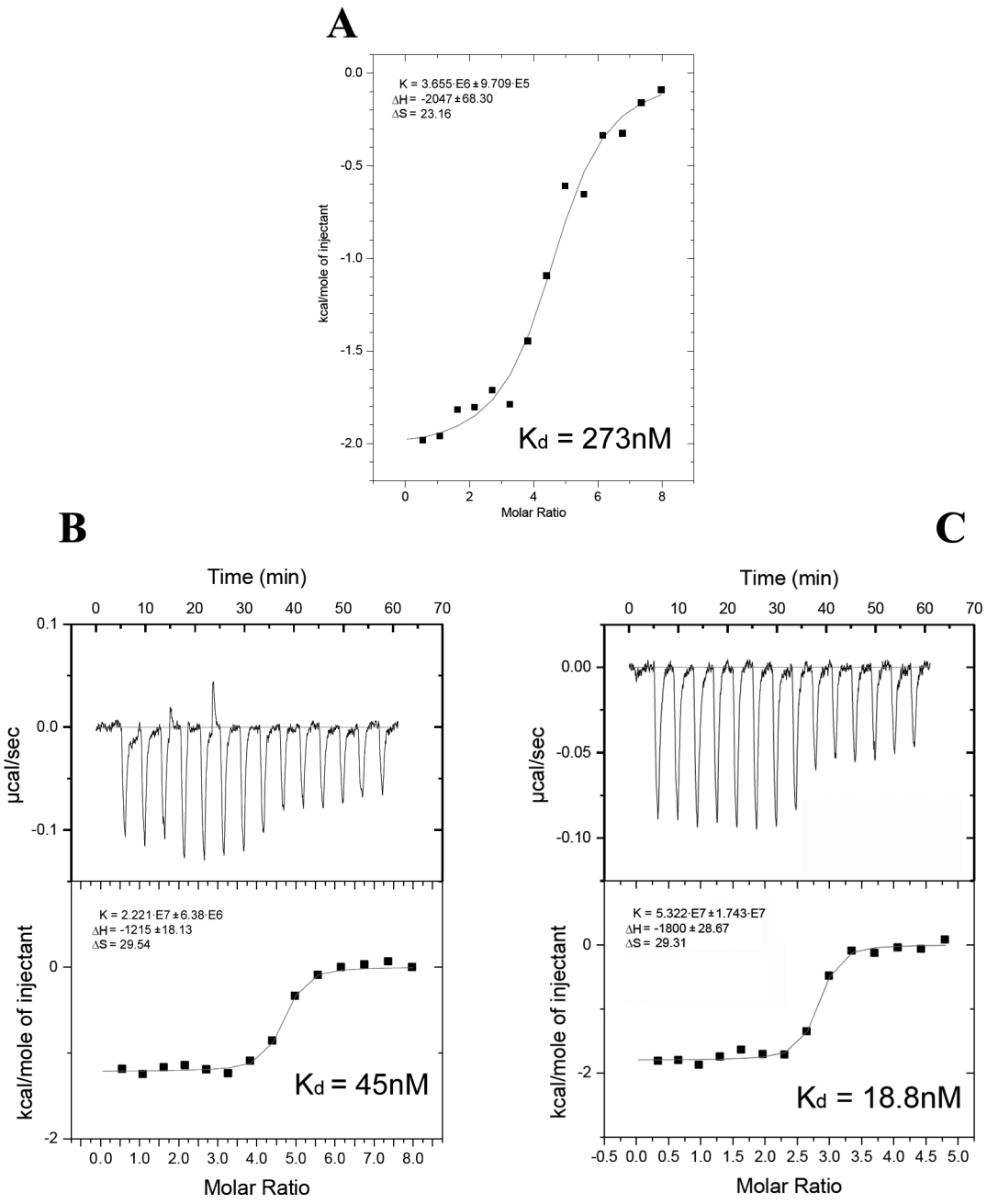

Figure 5. Isothermal titration calorimetry (ITC) profiles after titration of pentasaccharide (64 μM) (A), TMI (128 μM) (B), and pentasaccharide (64 μM) at saturating concentration of TMI (37 μM) (C) on a solution of antithrombin (3.44 μM).

Table 2. Rates of Inhibition of Thrombin and FXa by Antithrombin[a]

	k (μM^{-1} s^{-1})	
	thrombin	factor Xa
none	0.0035	0.0038
TMI	0.023 ± 0.0042	0.012 ± 0.0007
low affinity heparin	0.605 ± 0.0189	0.065 ± 0.0080
low affinity heparin + 1 μM TMI	0.683 ± 0.0536	0.087 ± 0.0066
high affinity heparin	5.023 ± 0.0012	2.115 ± 0.0013
high affinity heparin + 1 μM TMI	3.278 ± 0.0025	2.280 ± 0.0017

[a]Results were obtained from two independent experiments done in triplicate.

produced from standard heparin by chemical or enzymatic cleavage, giving chains about one-third the size,[31] led to increased bioavailability and easier administration than standard heparin, but they are not entirely devoid of the side effects discussed above. The minimal antithrombin binding pentasaccharide sequence (fondaparinux),[32] another recently discussed alternative, lacks an effective antidote to reverse excessive anticoagulation, and it has also been associated with bleeding.[33,34]

The ability of structure-based drug discovery to predict affinities crucially depends on the accuracy of the structural model of the complex. In the present study, we used the FlexScreen receptor−ligand docking approach[35,36] with a particular emphasis on screening efficiency in order to identify new molecules able to interact with the heparin binding domain

dx.doi.org/10.1021/jm300621j | J. Med. Chem. 2012, 55, 6403−6412

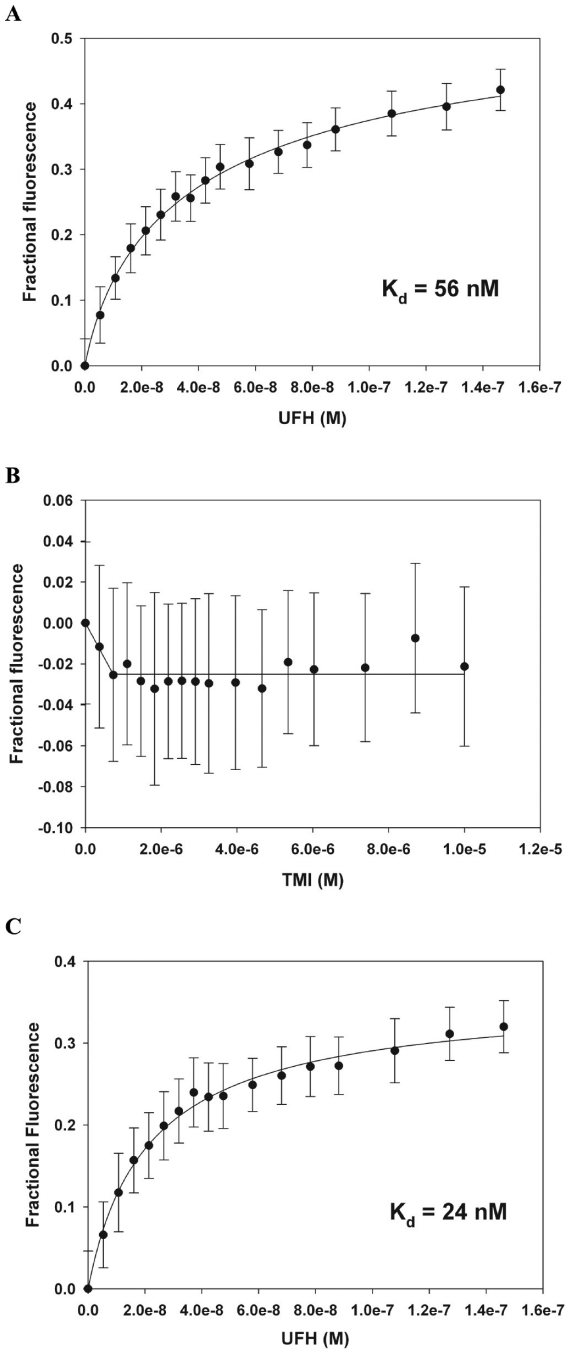

Figure 6. Fluorescence emission of antithrombin at 340 nm profiles after titration of UFH (A), TMI (B), and UFH at saturating concentration of TMI (37 μM) (C). Fractional fluorescence is the mean mean of at least 50 measurements.

of antithrombin. Sampling side chain conformations during the docking simulation were previously shown to improve scoring and docking of model systems.[37] FlexScreen describes interactions of the selected compounds with antithrombin mainly in terms of strong electrostatic and hydrogen bonds interactions, which makes antithrombin an ideal target for this approach. There is a reasonable correlation between total score and experimental K_d values for both TMI and heparin. The electrostatic parametrization[38] assigns higher negative charge density for oxygen in the following order: $PO_4 > SO_4 > SO_3 > CO_2$. This might explain why TMI, with a smaller number of

Table 3. Consequences of PAD Citrullination of Antithrombin (AT) (15 min at 37 °C) on the Anti-FXa Activity[a]

	% anti-FXa activity
AT	ref (100%)
AT + PAD	99.4 ± 1.2
AT + PAD + LMWH	30.0 ± 0.3
AT + PAD + TMI	30.0 ± 0.5

[a]Relevance of interaction with LMWH (140 μM) or with TMI (14.8 μM). Results, obtained from two independent experiments done in triplicate, were represented as % of the activity observed in samples only with antithrombin.

Table 4. Effect of TMI on Antithrombin Activity of Plasma of Healthy Subjects and One Homozygous Patient for the L99F Mutation, Causing a Type II Antithrombin Deficiency[a]

		% antithrombin activity	
plasma	TMI	UFH	Py-4-1
control	−	ref (100%)	ref (100%)
control	+	97.34 ± 2.70	101.4 ± 0.1
patient	−	33.22 ± 2.93	33.2 ± 2.9
patient	+	40.05 ± 4.19	37.2 ± 0.8

[a]The assay was done with an external supply of 1 μM UFH or over a confluent layer of Py-4-1 endothelial cells. Results, represented as the mean ± SD of two independent experiments performed in triplicate, were represented as % of the activity observed in control plasma without TMI.

charged groups than heparin (Table 1) but with higher overall negative charge density, interacts more strongly with antithrombin. Analogously 1,2,4-benzenetricarboxylic acid yields poorer interaction because its carboxyl groups carry a smaller charge. We observe for the different compounds (see Table 1) that a higher number of hydrogen bonds also correlates clearly with the predicted binding energy and experimental K_d value, although this interaction contributes less than electrostatic interactions to the overall estimated biding energy.

The main outcome of our study is the identification and experimental validation of a novel compound with high affinity to antithrombin, which features an as yet undocumented scaffold for antithrombin binding (45 nM for TMI vs 273 nM for pentasaccharide according to the ITC data). We found that TMI, in contrast to heparin, does not fully activate antithrombin (Figure 6), which results in only slightly increased rates of inhibition of thrombin and FXa. As heparin binding is known to induce a conformational change activating antithrombin, this smaller effect may be related to the differences in the binding poses between TMI and heparin and in their interactions in regions of antithrombin that are critical to induce the required conformational changes established for antithrombin activation.[39] As detailed in Table 1, TMI is missing the interaction with R13, R129, and R132. Several sequential conformational changes are required for full activation of antithrombin, which are initiated by a weak interaction of heparin with residues R129, K125, K11, and R13.[39] This initial interaction provokes a conformational change that enables binding to residues K114 and R47, which results in an enhancement of the initial interaction by an induced fit effect.[39] These conformational changes result in the complete exposition of the reactive center loop for the optimal

dx.doi.org/10.1021/jm300621j | J. Med. Chem. 2012, 55, 6403−6412

interaction of antithrombin with its target proteases. Exploration of the binding poses of TMI suggests that this complete cycle cannot be completed, failing to fully activated antithrombin, even though binding to residues K11, R46, R47, K114, and K125 induce a conformational change that facilitates the interaction with the proteases and enhances the interaction of antithrombin with heparin (Figures 5 and 6). Moreover, TMI also exposes the P1 residue of antithrombin (Arg393), allowing its citrullination at similar rates than for heparin alone (Table 2).[22] Combined, these data suggest that TMI induces a partially activated conformation,[20] which may generate a conformational change to facilitate the first step of the heparin binding.[40] Consequently combination of TMI and heparin increases the affinity of heparin for antithrombin, as experimentally verified by intrinsic fluorescence and ITC. TMI thus acts as a cofactor for heparin, provoking a synergistic effect rather than competition between both molecules. This may be particularly important for low affinity heparins, which are more abundant but had lower anticoagulant activity than high affinity heparins on vascular endothelium.

The minor activation of antithrombin combined with the higher heparin affinity induced by TMI and the absence of conformational side effects or negligible consequences on thrombin suggest a potential for TMI on the road toward new anticoagulant drugs. It is particularly challenging to ameliorate the hypercoagulable state of patients with antithrombin type II deficiency with heparin binding defect (Table 3),[41] where treatment with heparin would be inefficient.

EXPERIMENTAL SECTION

FlexScreen. Docking simulations have been performed with the all-atom FlexScreen receptor−ligand docking program,[35,36] which employs a force-field-based scoring function

$$S = \sum_{i,j}\left(\frac{R_{ij}}{r_{ij}^{12}} - \frac{A_{ij}}{r_{ij}^{6}} - \frac{q_i q_j}{\varepsilon r_{ij}}\right) + \sum_{\text{H-bonds}} \cos(\Theta_{ij})\left(\frac{\tilde{R}_{ij}}{r_{ij}^{12}} - \frac{\tilde{A}_{ij}}{r_{ij}^{10}}\right) \quad (1)$$

similar to that of AutoDock.[42] The scoring function contains Lennard-Jones (first two terms), electrostatic Coulomb (third term, $\varepsilon = 4$), and angular dependent hydrogen bond (terms 4 and 5) potentials. Protein and ligand atoms (i,j) are treated on the same footing. The Lennard-Jones and the hydrogen bond parameters have been taken from OPLSAA[43] and AutoDock,[42] respectively. The scoring function does not include solvent-related effects; it will thus differentiate between ligands where the binding energy is dominated by electrostatic/hydrogen bonding interactions and not by solvation contributions.

The docking protocol[35,36,44−47] was automated in order to consider all targets on the same footing. In addition to the protein and ligand structure (in the MOL2 format), FlexScreen requires a specification of a "docking center" (around which sampling is enhanced but that has no effect on the energies).

The ligands are docked using a cascadic version of the stochastic tunneling algorithm,[35,36,45,46] which samples translations of the center of mass and random rotations of the ligand, as well as intramolecular conformational changes of the ligands. If selected, the dihedral angles of several receptor side chains are also sampled (manual selection in the input). In each step FlexScreen either changes a dihedral angle of the ligand or a flexible side chain by a small, randomly chosen angle (drawn from a Gaussian distribution) or displaces the ligand by a small amount.[48] The total number of simulation steps was divided to three partitions: In the first partition 200 simulations (5000 steps each) were performed, the best 5 (by energy) were selected as the starting points of the second stage. After an additional 30 000 steps for each conformation in the second stage, the best two are selected for a final relaxation of 75 000 steps. The FlexScreen procedure thus generates two final conformations/energies for each ligand, providing an error estimate, and the conformation finally selected is the one with the lowest scoring function value. We also tested simulations with twice the number of steps but found no notable difference in results.

FlexScreen allows continuous rotations around the single bonds of the side chains of up to 15 residues in the energy optimization procedure.[45,46] For all parameters not explicitly stated default values were used. Depending on the number of ligand atoms and the number of flexible residues each ligand required from 1 to 3 min for rigid and to 5−15 min for flexible receptor docking (IntelPC-86-64, 1.8 GHz processor).

Receptor Structures. The model chosen for the receptor was obtained from PDB database with code 1AZX. It consists of a complex between active antithrombin and thrombin. Water molecules were removed and protonation states and receptor partial charges were prepared with the MOE, version 2003.02, program (Chemical Computing Group Inc., Montreal, Canada) using AMBER99 parameters.[49]

ZINC Database and Ligand Library. Ligand database files were downloaded from the ZINC database[16] in mol2 format. Hydrogens were added and partial charges calculated as described previously. Database was split into individual chunk files using Openbabel. Once molecule files were ready for calculations, they were uploaded to the different supercomputing resources provided by DEISA (http://www.deisa.eu/science/deci/projects2010-2011/BLOODINH), Cesga (Supercomputing Center of Galicia), and Karlsruhe Institute of Technology.

Surface Screening. In our blind docking surface screening approach, docking is performed for various different locations that cover the whole protein structure. A compromise must be found between number of points and computational cost, since increasing the number of points increases surface coverage but also computational cost.

We used a procedure where we selected all residues that belong to the protein surface using in-house PyMOL (Molecular Graphics System, version 1.3, Schrödinger, LLC) scripts, then use the coordinates of the α carbon of each residue, and finally specify a 5 Å cutoff for the docking simulation, i.e., different conformers will be generated into a 5 Å sphere, where the docking simulation will start from.

Reagents. Purified human antithrombin was obtained from commercial concentrates (Kybernin-P, ZLB Behring, Germany). LMWH (bemiparine, with a size of 3600 Da) and UFH (with an average size of 20 000 Da) were obtained from Laboratorios Rovi (Spain). Pentasaccharide (Fondaparinux with 1728 Da) was obtained from Arixtra (GSK, U.K.). Low affinity heparin was kindly supplied by Dr. James Huntington (CIMR, Cambridge, U.K.). 1,2,4-Benzenetricarboxylic acid was obtained from Sigma (Spain). Tetrapotassium 2,5-bis[(4-sulfonatophenyl)diazenyl]benzene-1,3-disulfonate was obtained from LookChemical (China). D-Myo-inositol 3,4,5,6-tetrakisphosphate (TMI) was obtained from SiChem (Germany), and disodium 4-hydroxy-5-sulfonaphthalene-2,7-disulfonate was obtained from ChemBridge (U.S.).

Isothermal Titration Calorimetry. ITC experiments were performed at 25 °C using a MicroCal VP-ITC microcalorimeter. Ligands and antithrombin solutions were prepared in Tris-HCl (ionic strength $I = 0.15$) buffer (pH 7.4). Protein solution was placed in the calorimeter cell, and the ligand solution was placed into the syringe injector. The titrations involved the injection of 20 μL of 128 μM ligand solution into the 3.44 μM antithrombin solution, with a 240 s delay between injections.

Functional Assays. Antithrombin anticoagulant activity was assessed by using chromogenic methods. 500 nM antithrombin with 16.4 μM TMI was incubated with 5 nM thrombin for 5 min. Then 100 μM S-2238 was added. Thrombin hydrolyzes the chromogenic substrate S-2238, producing p-nitroaniline, whose emission was recorded at 405 nm using a plate reader for 5 min (Synergy HT, U.K.).

Fluorescence Studies. Equilibrium dissociation constants (K_d) for the antithrombin−heparin interaction were determined essentially as described previously.[50] Change in intrinsic fluorescence of

antithrombin (25−50 nm) upon titration of the UFH was monitored at 340 nm on a Hitachi F-4500 fluorescence spectrophotometer, with excitation at 280 nm and using bandwidths of 3.5 nm for both excitation and emission. All titrations were carried out at room temperature under physiological ionic strength (I = 0.15) in 20 mM $NaPO_4$, 100 mM NaCl, 0.1 mM EDTA, 0.1% polyethylene glycol 8000, pH 7.4. Fluorescence emission intensity was taken as the average of 100 measurements recorded at 1 s intervals for each addition of heparin. Data were fitted as previously described.[51] Titrations were also carried out with TMI and with heparin after incubation of antithrombin with TMI (37 μM).

In Vitro Citrullination of Antithrombin. Antithrombin (1 mg/mL purified from plasma of healthy subjects) was incubated with peptidyl arginine deiminase (PAD) (isoform IV) from rabbit skeletal muscle (Sigma, Spain) at a molar ratio of 50:1 (antithrombin/PAD) in the presence and absence of 140 μM LMWH or 14.8 μM TMI. The reaction was performed at 37 °C in 100 mM Tris-HCl, 5 mM $CaCl_2$, pH 7.4. Samples were withdrawn at 15 min, and the reactions were stopped by addition of 50 mM EDTA.

The effect of PAD on the anticoagulant function of antithrombin was determined by a chromogenic method. Anti-FXa assays were performed with heparin, bovine FXa, and S-2765 chromogenic substrate (IL, IZASA, Spain). The absorbance of the reaction was measured at 405 nm.

Electrophoretic Studies. Potential conformational effects of TMI on antithrombin were evaluated by immunoelectrophoretic analysis using 8% (w/v) polyacrylamide nondenaturing PAGE with and without 7 M urea, as previously described.[52]

Rates of Inhibition. Second-order association rate constants ($M^{-1}\cdot s^{-1}$) for inhibition of FXa and thrombin by antithrombin and its complexes with different heparins and/or TMI were evaluated essentially as previously described.[53] For these experiments, pseudo-first-order conditions were used. Briefly, 10 μL of protease (20 nM) was incubated with an equal volume of antithrombin (400 nM) so that the final concentration of antithrombin was 20-fold of the protease. The buffer was composed of 20 mM $NaPO_4$, 100 mM NaCl, 0.1 mM EDTA, 0.1% PEG 8000, 0.1% BSA, pH 7.4. Reactions were incubated between 15 s and 5 min at room temperature. At the end of the incubation period, reactions were quenched by the addition of 200 μL of 150 μM chromogenic substrate. The residual protease activity was measured from the initial rates of substrate hydrolysis monitored at 405 nm. For the heparin-catalyzed rates, 20 μL samples contained 0.4 μM antithrombin, 20 nM protease, and 0.001−1 μM heparin in the same buffer at room temperature, and the rates were measured at 405 nm over 60 s on a microplate reader (Synergy HT, Bioteck, U.K.), in the presence or absence of 1 μM TMI. For the TMI-catalyzed rates, the same conditions were used as for the heparin-catalyzed rates but using a range between 10 and 100 nM. Measurements were also carried out with low affinity heparin that was purified as previously described.[54] The pseudo-first-order rate constants (k_{obs}) were obtained from the slopes of the plots of the natural logarithm of residual protease activity versus time of incubation. Second-order rate constants for the uncatalyzed reactions were obtained by dividing the observed pseudo-first-order rate constant (k_{obs}) by the inhibitor concentration. Second-order rate constants, $k_{cat}/K_{m,}$ for the heparin-catalyzed reactions were taken as the slope of k_{obs} versus the total heparin concentration, since K_d under these conditions was always significantly less than the initial antithrombin concentrations.

Antithrombin Activity of Plasma Samples. Plasma (3 μL) of a patient with type II antithrombin deficiency with heparin binding domain defect, antithrombin Budapest III:L99F in homozygous state, was incubated with or without 148 μM TMI. Then 8.73 nM thrombin was added and the mixture was incubated for 5 min at 37 °C in the presence or absence of UFH (1.27 mM). Finally, 1 mM S-2238 was added and absorbance was measured at 405 nm.

Py-4-1 is a hemangioma derived endothelial cell line isolated from a transgenic mouse carrying the polyoma virus early region. The cell line was kindly supplied by Dr. A. Rouzaut (CIMA, Navarra, Spain). Cells were maintained in DMEM (Invitrogen) supplemented with 10% fetal bovine serum (Sigma) at 37 °C in a humidified atmosphere of 5% CO_2. Cells were continuously passaged at confluence after treatment with trypsin−ethylenediaminetetraacetic acid buffered solution for over 100 passages. Cells were plated at a density of 2.86 × 10^5 cells/cm^2 in 96-well dishes in DMEM containing serum.

■ ASSOCIATED CONTENT

Ⓢ Supporting Information

Western blots of antithrombin fractions. This material is available free of charge via the Internet at http://pubs.acs.org.

■ AUTHOR INFORMATION

Corresponding Author

*For J.C.: phone, 34-968-341990; e-mail, javier.corral@carm.es. For W.W.: phone, 49-721-60826386; e-mail, wolfgang.wenzel@kit.edu.

Author Contributions

‖These authors contributed equally.

Notes

The authors declare no competing financial interest.

■ ACKNOWLEDGMENTS

This work was supported by Grant SAF2009-08993; Fundación Mutua Madrileña Grant RD06/0014/0039; Grant 04515/GERM/06, the Deutsche Forschungsgemeinschaft (Grant WE 1863/14-1); and Marie Curie FP7 PEOPLE Grant "INSILICODRUGDISCOVER". We also acknowledge the use of the computational facilities provided through the DEISA (http://www.deisa.eu/science/deci/projects2010-2011/BLOODINH) call and awarded to the project BLOODINH, to the Supercomputing Center of Galicia, and to the program HPC-Europa2. H.P.-S. is postdoctoral researcher of the University of Murcia, Spain, and I.M.-M. is an investigator from Fundación para la Formación e Investigación Sanitarias de la Región de Murcia (FFIS). J.N.-F. and J.A.G. hold postdoctoral contracts Sara Borrell from ISCIII. The program FlexScreen is available from the authors upon request.

■ ABBREVIATIONS USED

TMI, D-myo-inositol 3,4,5,6-tetrakisphosphate; LMWH, low molecular weight heparin; UHF, unfractionated heparin; ITC, isothermal titration calorimetry; PAD, peptidyl arginine deiminase

■ REFERENCES

(1) Paikin, J. S.; Eikelboom, J. W.; Cairns, J. A.; Hirsh, J. New antithrombotic agents—insights from clinical trials. *Nat. Rev. Cardiol.* **2010**, *7*, 498−509.

(2) Huntington, J. A.; Read, R. J.; Carrell, R. W. Structure of a serpin−protease complex shows inhibition by deformation. *Nature* **2000**, *407*, 923−926.

(3) Stratikos, E.; Gettins, P. G. Formation of the covalent serpin−proteinase complex involves translocation of the proteinase by more than 70 Å and full insertion of the reactive center loop into beta-sheet A. *Proc. Natl. Acad. Sci. U.S.A.* **1999**, *96*, 4808−4813.

(4) de Agostini, A. I.; Watkins, S. C.; Slayter, H. S.; Youssoufian, H.; Rosenberg, R. D. Localization of anticoagulantly active heparan sulfate proteoglycans in vascular endothelium: antithrombin binding on cultured endothelial cells and perfused rat aorta. *J. Cell Biol.* **1990**, *111*, 1293−1304.

(5) Marcum, J. A.; Atha, D. H.; Fritze, L. M.; Nawroth, P.; Stern, D.; Rosenberg, R. D. Cloned bovine aortic endothelial cells synthesize anticoagulantly active heparan sulfate proteoglycan. *J. Biol. Chem.* **1986**, *261*, 7507−7517.

(6) Olson, S. T.; Björk, I. Regulation of thrombin activity by antithrombin and heparin. *Semin. Thromb. Hemostasis* **1994**, *20*, 373−409.
(7) Harenberg, J.; Wehling, M. Current and future prospects for anticoagulant therapy: inhibitors of factor Xa and factor IIa. *Semin. Thromb. Hemostasis* **2008**, *34*, 39−57.
(8) Beck, E. The Treatment of Thrombosis. In *Discoveries in Pharmacology*; Elsevier: Amsterdam, 1984.
(9) Henry, B. L.; Connell, J.; Liang, A.; Krishnasamy, C.; Desai, U. R. Interaction of antithrombin with sulfated, low molecular weight lignins: opportunities for potent, selective modulation of antithrombin function. *J. Biol. Chem.* **2009**, *284*, 20897−20908.
(10) Gunnarsson, G. T.; Desai, U. R. Hydropathic interaction analyses of small organic activators binding to antithrombin. *Bioorg. Med. Chem.* **2004**, *12*, 633−640.
(11) Pérez-Sánchez, H.; Wenzel, W. Optimization methods for virtual screening on novel computational architectures. *Curr. Comput.-Aided Drug Des.* **2011**, *7*, 44−52.
(12) Guerrero, G. D.; Pérez-Sánchez, H.; Wenzel, W.; Cecilia, J. M.; García, J. M. Effective parallelization of non-boonded interactions kernel for virtual screening on GPUs. *Adv. Intell. Soft Comput.* **2011**, *93*, 63−69.
(13) Ghosh, S.; Nie, A.; An, J.; Huang, Z. Structure-based virtual screening of chemical libraries for drug discovery. *Curr. Opin. Chem. Biol.* **2006**, *10*, 194−202.
(14) Klebe, G. Virtual ligand screening: strategies, perspectives and limitations. *Drug Discovery Today* **2006**, *11*, 580−594.
(15) Warren, G. L.; Andrews, C. W.; Capelli, A. M.; Clarke, B.; LaLonde, J.; Lambert, M. H.; Lindvall, M.; Nevins, N.; Semus, S. F.; Senger, S.; Tedesco, G.; Wall, I. D.; Woolven, J. M.; Peishoff, C. E.; Head, M. S. A critical assessment of docking programs and scoring functions. *J. Med. Chem.* **2006**, *49*, 5912−5931.
(16) Irwin, J. J.; Shoichet, B. K. ZINC—a free database of commercially available compounds for virtual screening. *J Chem. Inf. Model.* **2005**, *45*, 177−182.
(17) Shears, S. B. The versatility of inositol phosphates as cellular signals. *Biochim. Biophys. Acta* **1998**, *1436*, 49−67.
(18) Xie, W.; Kaetzel, M. A.; Bruzik, K. S.; Dedman, J. R.; Shears, S. B.; Nelson, D. J. Inositol 3,4,5,6-tetrakisphosphate inhibits the calmodulin-dependent protein kinase II-activated chloride conductance in T84 colonic epithelial cells. *J. Biol. Chem.* **1996**, *271*, 14092−14097.
(19) Traynor-Kaplan, A. E.; Moody, M.; Nur, M.; Gabriel, S.; Majerus, P. W.; Drumm, M. L.; Langton-Webster, B. INO-4995 therapeutic efficacy is enhanced with repeat dosing in cystic fibrosis knockout mice and human epithelia. *Am. J. Respir. Cell Mol. Biol.* **2010**, *42*, 105−112.
(20) Johnson, D. J.; Langdown, J.; Li, W.; Luis, S. A.; Baglin, T. P.; Huntington, J. A. Crystal structure of monomeric native antithrombin reveals a novel reactive center loop conformation. *J. Biol. Chem.* **2006**, *281*, 35478−35486.
(21) Pike, R. N.; Potempa, J.; Skinner, R.; Fitton, H. L.; McGraw, W. T.; Travis, J.; Owen, M.; Jin, L.; Carrell, R. W. Heparin-dependent modification of the reactive center arginine of antithrombin and consequent increase in heparin binding affinity. *J. Biol. Chem.* **1997**, *272*, 19652−19655.
(22) Ordóñez, A.; Martínez-Martínez, I.; Corrales, F. J.; Miqueo, C.; Miñano, A.; Vicente, V.; Corral, J. Effect of citrullination on the function and conformation of antithrombin. *FEBS J.* **2009**, *276*, 6763−6772.
(23) Hernández-Espinosa, D.; Ordóñez, A.; Vicente, V.; Corral, J. Factors with conformational effects on haemostatic serpins: implications in thrombosis. *Thromb. Haemostasis* **2007**, *98*, 557−563.
(24) Skinner, R.; Abrahams, J. P.; Whisstock, J. C.; Lesk, A. M.; Carrell, R. W.; Wardell, M. R. The 2.6 Å structure of antithrombin indicates a conformational change at the heparin binding site. *J. Mol. Biol.* **1997**, *266*, 601−609.
(25) Connolly, S. J.; Ezekowitz, M. D.; Yusuf, S.; Eikelboom, J.; Oldgren, J.; Parekh, A.; Pogue, J.; Reilly, P. A.; Themeles, E.; Varrone, J.; Wang, S.; Alings, M.; Xavier, D.; Zhu, J.; Diaz, R.; Lewis, B. S.; Darius, H.; Diener, H. C.; Joyner, C. D.; Wallentin, L. Dabigatran versus warfarin in patients with atrial fibrillation. *N. Engl. J Med.* **2009**, *361*, 1139−1151.
(26) Ma, T. K.; Yan, B. P.; Lam, Y. Y. Dabigatran etexilate versus warfarin as the oral anticoagulant of choice? A review of clinical data. *Pharmacol. Ther.* **2011**, *129*, 185−194.
(27) Conrad, H. E. *Heparin-Binding Proteins*; Academic Press: San Diego, CA, 1998.
(28) Devlin, V. J.; Einhorn, T. A.; Gordon, S. L.; Alvarez, E. V.; Butt, K. M. Total hip arthroplasty after renal transplantation. Long-term follow-up study and assessment of metabolic bone status. *J. Arthroplasty* **1988**, *3*, 205−213.
(29) Ten, C. H. Trombocytopenia: one of the markers of disseminated intravascular coagulation. *Pathophysiol. Haemostasis Thromb.* **2003**, *33*, 413−416.
(30) Warkentin, T. E.; Chong, B. H.; Greinacher, A. Heparin-induced thrombocytopenia: towards consensus. *Thromb. Haemostasis* **1998**, *79*, 1−7.
(31) Barrowcliffe, T. W. Low molecular weight heparin(s). *Br. J. Haematol.* **1995**, *90*, 1−7.
(32) Choay, J.; Petitou, M.; Lormeau, J. C.; Sinay, P.; Casu, B.; Gatti, G. Structure−activity relationship in heparin: a synthetic pentasaccharide with high affinity for antithrombin III and eliciting high anti-factor Xa activity. *Biochem. Biophys. Res. Commun.* **1983**, *116*, 492−499.
(33) Blick, S. K.; Orman, J. S.; Wagstaff, A. J.; Scott, L. J. Fondaparinux sodium: a review of its use in the management of acute coronary syndromes. *Am. J. Cardiovasc. Drugs* **2008**, *8*, 113−125.
(34) Janin, S.; Meneveau, N.; Mahemuti, A.; Descotes-Genon, V.; Dutheil, J.; Chopard, R.; Seronde, M. F.; Schiele, F.; Bernard, Y.; Bassand, J. P. Safety and efficacy of fondaparinux as an adjunctive treatment to thrombolysis in patients with high and intermediate risk pulmonary embolism. *J. Thromb. Thrombolysis* **2009**, *28*, 320−324.
(35) Merlitz, H.; Wenzel, W. Comparison of stochastic optimization methods for receptor−ligand docking. *Chem. Phys. Lett.* **2002**, *362*, 271−277.
(36) Merlitz, H.; Burghardt, B.; Wenzel, W. Application of the stochastic tunneling method to high throughput database screening. *Chem. Phys. Lett.* **2003**, *370*, 68−73.
(37) Merlitz, H.; Burghardt, B.; Wenzel, W. Impact of receptor conformation on in silico screening performance. *Chem. Phys. Lett.* **2004**, *390*, 500−505.
(38) Cornell, W. D.; Cieplak, P.; Bayly, C. I.; Gould, I. R.; Merz, K. M.; Ferguson, D. M.; Spellmeyer, D. C.; Fox, T.; Caldwell, J. W.; Kollman, P. A. A second generation force field for the simulation of proteins, nucleic acids, and organic molecules. *J. Am. Chem. Soc.* **1995**, *117*, 5179−5197.
(39) Olson, S. T.; Chuang, Y. J. Heparin activates antithrombin anticoagulant function by generating new interaction sites (exosites) for blood clotting proteinases. *Trends Cardiovasc. Med.* **2002**, *12*, 331−338.
(40) Schedin-Weiss, S.; Richard, B.; Olson, S. T. Kinetic evidence that allosteric activation of antithrombin by heparin is mediated by two sequential conformational changes. *Arch. Biochem. Biophys.* **2010**, *504*, 169−176.
(41) Simmonds, R. E.; Hermida, J.; Rezende, S. M.; Lane, D. A. Haemostatic genetic risk factors in arterial thrombosis. *Thromb. Haemostasis* **2001**, *86*, 374−385.
(42) Morris, G. M.; Goodsell, D. S.; Halliday, R.; Huey, R.; Hart, W. E.; Belew, R. K.; Olson, A. J. Automated docking using a Lamarckian genetic algorithm and an empirical binding free energy function. *J. Comput. Chem.* **1998**, *19*, 1639−1662.
(43) Jorgensen, W. L.; McDonald, N. A. Development of an all-atom force field for heterocycle. Properties liquid pyridine and diazenes. *J. Mol. Struct.* **1998**, *424*, 145−155.
(44) Fischer, B.; Merlitz, H.; Wenzel, W. Increasing diversity in in-silico screening with target flexibility. *Lect. Notes Comput. Sci.* **2005**, *3695*, 186−197.

(45) Wenzel, W.; Hamacher, K. Stochastic tunneling approach for global minimization of complex potential energy landscapes. *Phys. Rew. Lett.* **1999**, *82*, 3003−3007.
(46) Merlitz, H.; Wenzel, W. High throughput in-silico screening against flexible protein receptors. *Lect. Notes Comput. Sci.* **2004**, *3045*, 465−472.
(47) Fischer, B.; Basili, S.; Merlitz, H.; Wenzel, W. Accuracy of binding mode prediction with a cascadic stochastic tunneling method. *Proteins* **2007**, *68*, 195−204.
(48) Rabal, O.; Schneider, G.; Borrell, J. I.; Teixido, J. Structure-based virtual screening of FGFR inhibitors: cross-decoys and induced-fit effect. *BioDrugs* **2007**, *21*, 31−45.
(49) Wang, J.; Cieplak, P.; Kollman, P. A. How well does a restrained electrostatic potential (RESP) model perform in calculating conformational energies of organic and biological molecules? *J. Comput. Chem.* **2000**, *21*, 1049−1074.
(50) Martínez-Martínez, I.; Ordoñez, A.; Navarro-Fernández, J.; Pérez-Lara, A.; Gutiérrez-Gallego, R.; Giraldo, R.; Martínez, C.; Llop, E.; Vicente, V.; Corral, J. Antithrombin Murcia (K241E) causing antithrombin deficiency: a possible role for altered glycosylation. *Haematologica* **2010**, *95*, 1358−1365.
(51) Langdown, J.; Belzar, K. J.; Savory, W. J.; Baglin, T. P.; Huntington, J. A. The critical role of hinge-region expulsion in the induced-fit heparin binding mechanism of antithrombin. *J. Mol. Biol.* **2009**, *386*, 1278−1289.
(52) Beauchamp, N. J.; Pike, R. N.; Daly, M.; Butler, L.; Makris, M.; Dafforn, T. R.; Zhou, A.; Fitton, H. L.; Preston, F. E.; Peake, I. R.; Carrell, R. W. Antithrombins Wibble and Wobble (T85M/K): archetypal conformational diseases with in vivo latent-transition, thrombosis, and heparin activation. *Blood* **1998**, *92*, 2696−2706.
(53) Olson, S. T.; Swanson, R.; Raub-Segall, E.; Bedsted, T.; Sadri, M.; Petitou, M.; Herault, J. P.; Herbert, J. M.; Björk, I. Accelerating ability of synthetic oligosaccharides on antithrombin inhibition of proteinases of the clotting and fibrinolytic systems. Comparison with heparin and low-molecular-weight heparin. *Thromb. Haemostasis* **2004**, *92*, 929−939.
(54) Streusand, V. J.; Björk, I.; Gettins, P. G.; Petitou, M.; Olson, S. T. Mechanism of acceleration of antithrombin−proteinase reactions by low affinity heparin. Role of the antithrombin binding pentasaccharide in heparin rate enhancement. *J. Biol. Chem.* **1995**, *270*, 9043−9051.